

AAL881, a Novel Small Molecule Inhibitor of RAF and Vascular Endothelial Growth Factor Receptor Activities, Blocks the Growth of Malignant Glioma

Sith Sathornsumetee,¹ Anita B. Hjelmeland,¹ Stephen T. Keir,¹ Roger E. McLendon,² David Batt,⁶ Timothy Ramsey,⁶ Naeem Yusuff,⁶ B.K. Ahmed Rasheed,² Mark W. Kieran,⁷ Andrea Laforme,⁷ Darell D. Bigner,^{1,2} Henry S. Friedman,^{1,2,3} and Jeremy N. Rich^{1,4,5}

Departments of ¹Surgery, ²Pathology, ³Pediatrics, ⁴Medicine, and ⁵Neurobiology, Duke University Medical Center, Durham, North Carolina; ⁶Novartis Institutes for Biomedical Research, Cambridge, Massachusetts; and ⁷Department of Pediatrics, Dana-Farber Cancer Institute, Boston, Massachusetts

Abstract

Malignant gliomas are highly proliferative and angiogenic cancers resistant to conventional therapies. Although RAS and RAF mutations are uncommon in gliomas, RAS activity is increased in gliomas. Additionally, vascular endothelial growth factor and its cognate receptors are highly expressed in gliomas. We now report that AAL881, a novel low-molecular weight inhibitor of the kinase activities associated with B-RAF, C-RAF (RAF-1), and VEGF receptor-2 (VEGFR2), showed activity against glioma cell lines and xenografts. In culture, AAL881 inhibited the downstream effectors of RAF in a concentration-dependent manner, with inhibition of proliferation associated with a G₁ cell cycle arrest, induction of apoptosis, and decreased colony formation. AAL881 decreased the proliferation of bovine aortic endothelial cells as well as the tumor cell secretion of vascular endothelial growth factor and inhibited the invasion of glioma cells through an artificial extracellular matrix. Orally administered AAL881 was well tolerated with minimal weight loss in non-tumor-bearing mice. Established s.c. human malignant glioma xenografts grown in immunocompromised mice treated with a 10-day course of oral AAL881 exhibited growth delays relative to control tumors, frequently resulting in long-term complete regressions. AAL881 treatment extended the survival of immunocompromised mice bearing orthotopic glioma xenografts compared with placebo controls. The intraparenchymal portions of orthotopic AAL881-treated tumors underwent widespread necrosis consistent with vascular disruption compared with the subarachnoid elements. These effects are distinct from our prior experience with VEGFR2 inhibitors, suggesting that targeting RAF itself or in combination with VEGFR2 induces profound tumor responses in gliomas and may serve as a novel therapeutic approach in patients with malignant gliomas. (Cancer Res 2006; 66(17): 8722-30)

Introduction

Malignant gliomas are highly lethal tumors despite maximal therapy (1). Conventional therapies rely on DNA damage or disruption of mitosis in a nonspecific fashion. The elucidation of

molecular alterations underlying the development of gliomas has provided the theoretical basis of novel therapeutic approaches. Several current therapeutic targets represent components of oncogenic signal transduction pathways that are inappropriately activated in a broad range of gliomas (2). Most targeted therapeutic studies in gliomas to date have involved inhibitors of growth factor receptors, but less clear to glioma growth are the relative contributions of intracellular signaling elements that regulate key cellular behaviors involved in tumorigenesis. The RAS family members are small GTPases that stimulate proliferation, invasion, and secretion of angiogenic factors through activation of downstream effectors including RAF family members (2). Despite the lack of activating mutations of RAS family members in central nervous system tumors (3–6), RAS activity is increased in many gliomas through the activation of upstream growth factor receptors including epidermal growth factor receptor (EGFR) and platelet-derived growth factor receptor (PDGFR; refs. 7–9). The contributions of RAS in glioma formation have been dissected in several studies of genetically defined human and murine glioma models in which oncogenic RAS can drive gliomagenesis (10–13). The RAS pathway has been targeted therapeutically through the use of farnesyltransferase inhibitors (FTI) that disrupt the rate-limiting posttranscriptional step of RAS. The selectivity of the effects of FTIs to RAS is questionable, but FTIs have shown modest activity against gliomas in both preclinical and clinical trials (14–20). These results suggest that the RAS pathway represents a useful therapeutic target for malignant gliomas. As the RAF proteins are kinases that are key downstream effectors of RAS family members which positively regulate tumorigenesis, we expected that RAF might represent an additional glioma treatment target. RAF kinases are serine/threonine kinases that activate mitogen-activated protein kinase kinases (MEK) with positive transcriptional regulation of key cellular genes that drive cell cycle progression. Although the activity of another downstream pathway of RAS—phosphatidylinositol 3-kinase (PI3K)—has been associated with poor prognosis in patients with glioma and is the target of novel brain tumor therapies (21), relatively less is known about the specific contributions of RAF to gliomas. A subset of malignant gliomas has detectable activating mutations in the B-RAF gene (22–24), suggesting that these tumors may exhibit constitutive activity mediated by RAF.

In this study, we sought to determine the effect of blocking RAF activity with a novel low-molecular weight RAF kinase inhibitor in a well-characterized human glioma model. AAL881 is an orally available low-molecular weight ATP-mimetic inhibitor of the kinase activity of B-RAF, C-RAF, and vascular endothelial growth

Requests for reprints: Jeremy N. Rich, Preston Robert Tisch Brain Tumor Center, Duke University Medical Center, Box 2900, Durham, NC 27710. Phone: 919-681-1693; Fax: 919-684-6514; E-mail: rich0001@mc.duke.edu.

©2006 American Association for Cancer Research.
doi:10.1158/0008-5472.CAN-06-0284

factor receptor-2 (VEGFR2; KDR/Flk-1). As small molecule inhibitors of VEGFR kinases have shown limited activity in both preclinical and clinical glioma studies, we hypothesized that targeting both upstream angiogenic growth factor receptors and a key mediator of cellular proliferation may offer therapeutic advantage. We now show significant efficacy of AAL881 against malignant glioma in both *in vitro* and *in vivo* murine models of human xenografts.

Materials and Methods

Cells and culture. THR is a genetically defined human glioma cell line that we developed based on the serial introduction of SV40 early T antigen, human telomerase catalytic subunit, and an oncogenic Harvey-Ras (10). The U87MG, T98G, and U373MG human glioma cell lines were purchased from the American Type Culture Collection (Manassas, VA). The U251MG cell line was a generous gift from J. Ponten, University of Uppsala, Sweden. The D423MG, D566MG, and D645MG glioma lines were derived from human glioma biopsy specimens. The well-characterized human malignant glioma xenograft, D54MG, is the Duke University subline of A-172. D54MG, U87MG, and U373MG cells were maintained by culturing in 10-cm tissue culture dishes in Zinc Option medium containing 10% fetal bovine serum (Life Technologies, Grand Island, NY) and glutamine (Life Technologies) until ready for use.

Drugs. AAL881 was generously provided by Novartis Institutes for Biomedical Research (Cambridge, MA). Ten millimole stock solutions were dissolved in DMSO (Sigma-Aldrich, St. Louis, MO), stored at -80°C , and diluted in fresh medium immediately before use.

Western blot analysis. Cells were placed in serum-free Zinc Option media for 24 hours before experiments, treated with either DMSO control, or increasing concentrations of AAL881 for 2 hours, stimulated with serum for 10 minutes, lysed in lysis buffer [62.5 mmol/L Tris-HCl, 2% w/v SDS, 10% glycerol, and 40 mmol/L DTT], with protease and phosphatase inhibitors, vortexed for 5 seconds, and centrifuged at 14,000 rpm for 5 minutes at 4°C . An equal amount of protein was resolved by SDS-PAGE, transferred to polyvinylidene difluoride membranes (Millipore, Billerica, MA), and detected using an enhanced chemiluminescence system (Pierce Biotechnology, Rockford, IL). Phosphospecific B-RAF, phosphospecific C-RAF, total A-RAF, total B-RAF, and total C-RAF antibodies were purchased from Santa Cruz Biotechnology, Inc. (Santa Cruz, CA). Phosphospecific extracellular signal-regulated kinase 1/2 (ERK1/2) and total ERK1/2 antibodies were purchased from Promega (Madison, WI). Phosphospecific MEK1/2 (MAP2K1), phosphospecific AKT (Ser⁴⁷³), total MEK1/2, and total AKT antibodies were purchased from Cell Signaling Technology (Beverly, MA). Anti- α -TUBULIN was purchased from Sigma-Aldrich. Antibodies were used according to the manufacturer's instructions.

Thymidine incorporation assay. Cells were plated into 12-well plates at a density of 1×10^4 cells/well, serum-starved overnight, and then treated with DMSO or various concentrations of AAL881 for 48 hours in 10% serum. For the last 4 hours of culture, cells were labeled with 4 μCi of [³H]thymidine. Cells were then washed, fixed in 10% trichloroacetic acid, and lysed in 0.2 N NaOH. [³H]-Thymidine incorporation into the DNA was measured with a scintillation counter. Each data point is the average of quadruplicates.

Vascular endothelial growth factor quantification. Vascular endothelial growth factor (VEGF) Quantikine Assay kit was purchased from R&D Systems (Minneapolis, MN). D54MG cells were serum-starved for 24 hours, and then treated with 0.1% DMSO control, or increasing concentrations of AAL881 for 48 hours in serum-free medium. Supernatants were collected and ELISA assays were done according to the manufacturer's instructions. Plates were read for absorbance on VESAMax plate scanner set to 450 nm with wavelength correction at 540 nm.

Bovine aortic endothelial cell assay. Bovine aortic endothelial proliferation was done as previously described (25).

Flow cytometric and Annexin V analyses. Two hundred thousand cells were plated into 10-cm tissue culture dishes, serum-starved overnight, and

treated with either DMSO control or 5 $\mu\text{mol/L}$ of AAL881 in Zinc Option medium containing 10% fetal bovine serum for 48 hours. The cells were then removed from the plate, fixed in ethanol, and stained with propidium iodide. Analysis was done on FACScan, gated to exclude cellular debris, and collecting 10^4 events. Calculations were done using BD software. For Annexin V analysis, 100,000 cells were plated in six-well plates, serum-starved overnight with either DMSO control or 5 $\mu\text{mol/L}$ of AAL881, collected for analysis, washed twice with Dulbecco's PBS, and stained with propidium iodide and Annexin V (BD PharMingen, San Diego, CA) according to the manufacturer's instructions.

Colony formation assays. Five hundred cells were plated in each well of a six-well plate in sextuplicate in medium with 10% serum. The next day, either DMSO control or AAL881 diluted in equal amounts of final volumes of DMSO was added. After 10 days of incubation, the cells were fixed and stained with Coomassie blue (0.1%) for 10 minutes and washed thoroughly in distilled water.

Migration/invasion assays. Kits were purchased from BD Biosciences (San Jose, CA) and used according to the manufacturer's instructions. Cells were treated with either DMSO control or increasing concentrations of AAL881 in serum-free medium for 24 hours. Treated cells were trypsinized, washed, counted, and resuspended in serum-free medium to a concentration of 50,000 cells/mL. Cells were treated with DMSO control or the indicated concentrations of AAL881 and 500 μL (25,000 cells) were placed in the upper chamber of inserts uncoated (migration) or coated with Matrigel (invasion). The bottom chamber was filled with 500 μL of Zinc Option medium containing 10% fetal bovine serum as a chemoattractant. After 48 hours, the migration inserts were fixed and stained with Diff-Quik solutions. All invaded cells were counted manually for the entire membrane. Invasion was calculated as a ratio of cells observed in control (uncoated) inserts to those observed in Matrigel-coated inserts. Experiments were done in triplicate.

Statistical analysis of *in vitro* studies. All quantitative data are presented with means \pm SEs. Significance was determined by two-tailed Student's *t* test with $\alpha = 0.05$.

Intracranial xenograft studies. Athymic male BALB/c *nu/nu* mice were maintained in high-efficiency particulate air-filtered facilities in the Duke University Cancer Center Isolation Facility according to institutional policy approved by the Duke Institutional Animal Care and Use Committee. For intracranial model studies, xenografts passaged in athymic mice were excised, minced, and cells separated with a cytosieve into Zinc Option solution. After centrifugation, supernatant was removed, and cells were mixed 1:1 with methylcellulose. Total homogenate (10 μL) was then injected with a Hamilton syringe (Hamilton, Co., Reno, NV) into the brains of athymic male BALB/c *nu/nu* mice. For intracranial tumor therapy, groups of 10 mice were randomized 1 day after intracranial tumor implantation. AAL881 was then administered at a dose of 100 mg/kg q.d. by oral gavage for a total of 10 days (5 days on/2 days off/5 days on). Animals were observed twice daily for signs of distress or development of neurologic symptoms, at which time, the mice were sacrificed. The response of the intracranial xenograft studies was assessed as the difference in the median duration of survival until neurologic deterioration.

S.c. xenograft transplantation. Athymic male BALB/c *nu/nu* mice were maintained in high-efficiency particulate air-filtered facilities in the Duke University Cancer Center Isolation Facility according to institutional policy approved by the Duke Institutional Animal Care and Use Committee. For s.c. tumor transplantation, s.c. xenografts passaged in athymic mice were excised, minced, and separated with a tissue press. Fifty microliters of homogenate were injected into the right flank of each mouse with a Hamilton syringe (26). For s.c. tumor therapy, groups of 10 athymic male BALB/c *nu/nu* mice randomly selected based on tumor volume were treated when the median tumor volume was in the range of 100 to 300 mm^3 , and were compared with control animals receiving drug vehicle. AAL881 was administered at a dose of 100 mg/kg q.d. by oral gavage for a total of 10 days (5 days on/2 days off/5 days on). Tumors were measured twice weekly with hand-held vernier calipers (Scientific Products, McGraw, IL). Tumor volume was calculated according to the following formula: $V = [(\text{width})^2 \times (\text{length})] / 2$. The response of the s.c. xenografts was assessed by

delay in tumor growth and by tumor regression. Growth delay, expressed as $T - C$, is defined as the difference in days between the median time required for tumors in treated (T) and control (C) animals to reach a volume five times greater than that measured at the start of treatment. Partial tumor regression is defined as a decrease in tumor volume over at least two successive measurements.

Drug tolerability. Mice were weighed twice weekly and were checked at least twice daily for general clinical condition.

Statistical analysis of *in vivo* data. Statistical analyses were done using a personalized SAS statistical analysis program, the Wilcoxon rank order test for growth delay, and Fisher's exact test for tumor regression, as described previously (26). Survival estimates and median survivals were determined by using the method of Kaplan and Meier.

Immunohistochemistry. Athymic nude mice with established orthotopic D54MG intracranial xenografts were treated daily with vehicle control (DMSO) or AAL881 (100 mg/kg per gavage) for 10 days (5 days on/2 days off/5 days on). Tumors were harvested simultaneously and portions were fixed in 10% buffered formalin for 24 hours and transferred to 70% ethanol, then sectioned for staining with H&E or immunohistologic analysis with antibodies against Ki-67, phospho-ERK1/2, and phospho-AKT. Phospho-specific ERK1/2 (T183 and Y185) antibody was purchased from Santa Cruz Biotechnology. An immunohistochemistry detection kit for phosphospecific AKT (Ser⁴⁷³) was purchased from Cell Signaling Technology and used according to the manufacturer's instructions.

Formalin-fixed, paraffin-embedded sections were used for analysis with antibodies directed against Ki-67, pERK1/2, and pAKT as has been previously described (27, 28). Immunoreactivity was graded by a neuropathologist blinded as to treatment protocols (R.E. McLendon). A semiquantitative score was derived from an intensity score of the reactivity product [absent (0), mild (1), moderate (2), and strong (3)] related to endogenous positive controls multiplied by a distribution score [focal (1), multifocal (2), and diffuse (3)] as described previously (29). All quantitative data are presented with means \pm SEs. Significance was determined by two-tailed Student's t test with $\alpha = 0.05$.

Results

Human glioma cell lines differentially express RAF proteins.

To validate the targeting of B-RAF and C-RAF in human glioma with AAL881, we first established that human glioma cell lines express RAF proteins. THR, D54MG, U87MG, U251MG, T98G, D645MG, D423MG, U373MG, and D566MG all expressed A-RAF, B-RAF, and C-RAF (Fig. 1), although the levels of protein expression varied between cell lines. Total levels of B-RAF were highest in D423MG, U373MG, and U87MG, whereas total levels of C-RAF were highest in U87MG, THR, and D645MG. Phosphorylated (activated) B-RAF was present in U87MG, U251MG, T98G, and D423MG cells, whereas D54MG, D645MG, U373MG, and D566MG cells displayed minimal activation of B-RAF. Activated C-RAF was highest in U87MG, followed by D54MG, U251MG, and THR cells, whereas low levels of active C-RAF were observed in T98G, D423MG, and U373MG. As AAL881 is a kinase inhibitor of both C-RAF and B-RAF, we used D54MG, U87MG, and U373MG human glioma cell lines which differentially express active B-RAF and C-RAF for *in vitro* experiments to evaluate the antineoplastic efficacy of AAL881.

AAL881 inhibits signal transduction downstream of RAF. To evaluate the ability of AAL881 to effectively target signal transduction pathways downstream of RAF, we examined the phosphorylation of components of the RAF/MAPK pathway in the presence and absence of serum and AAL881. As expected, serum induced the phosphorylation (activation) of MEK and ERK in serum-starved D54MG cells (Fig. 2A). Pretreatment with AAL881 prevented the phosphorylation of MEK and ERK in a concentra-

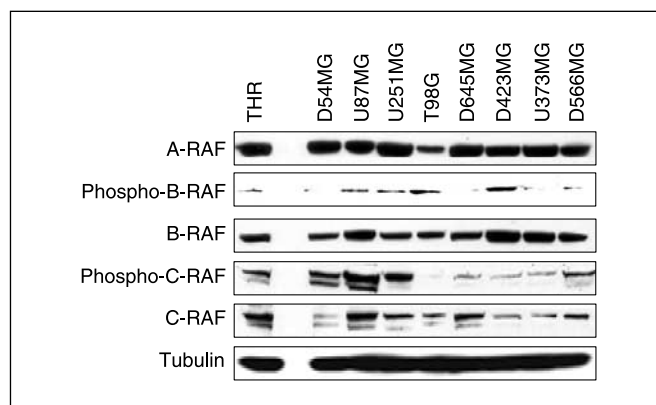


Figure 1. Glioma cell lines express differential levels and activation of RAF isoforms. Whole cell lysates were prepared from a genetically defined glioma line (THR) and a panel of human glioma cell lines derived from patient biopsy specimens. Total (A-RAF, B-RAF, and C-RAF) and active (B-RAF and C-RAF) isoforms of RAF were detected by Western analysis using appropriate antibodies. U87MG has the highest levels of active B-RAF and active C-RAF, whereas D54MG has high levels of active C-RAF and low levels of active B-RAF, whereas U373 has the lowest levels of active B-RAF and active C-RAF.

tion-dependent manner with 5 μ mol/L of AAL881 sufficient to significantly inhibit MEK and ERK phosphorylation without affecting total MEK or ERK levels. AAL881 also inhibited the serum-induced phosphorylation of AKT (Fig. 2A), a component of a parallel intracellular signal transduction pathway promoting cellular survival and resistance to apoptotic stimuli. As D54MG cells, like many human gliomas, express a nonfunctional form of PTEN (data not shown) that fails to inhibit the PI3K/AKT pathway, the AKT signaling pathway and its downstream elements are likely more active in D54MG cultures than in normal human tissue. Thus, AAL881 can target key intracellular oncogenic pathways that contribute to glioma pathophysiology.

AAL881 inhibits glioma cell proliferation. To determine the effect of AAL881 on glioma cell proliferation, thymidine incorporation was assessed in D54MG, U87MG, and U373MG cells in the presence and absence of AAL881. In D54MG and U87MG, 10 μ mol/L of AAL881 was required to significantly inhibit cell proliferation by 79% and 36%, respectively (Fig. 2B). In U373MG, a significant reduction in thymidine incorporation was observed with 5 μ mol/L of AAL881 which reduced cell proliferation by 38%. Treatment of U373MG cells with 10 μ mol/L of AAL88 led to a 68% reduction in thymidine incorporation (Fig. 2B). These data indicate that although AAL881 was capable of inhibiting the proliferation of all three glioma cell lines tested, sensitivity to the antiproliferative effects of AAL881 varied. A 50% reduction in thymidine incorporation in D54MG and U373MG cells required an AAL881 concentration between 5 and 10 μ mol/L, whereas 10 to 15 μ mol/L was necessary for a similar reduction in U87MG cells. This necessity for higher concentrations of AAL881 in U87MG compared with D54MG or U373MG may be due to the higher levels of activated B-RAF and C-RAF observed in U87MG cells (Fig. 1).

An essential aspect of tumor cell proliferation involves the ability of tumor cells to promote cell proliferation in the absence of external mitogenic stimuli. As further evidence of the antiproliferative effects of AAL881, we showed that the colony formation of D54MG, U373MG, and U87MG cells was inhibited in a concentration-dependent manner by AAL881 (Fig. 2C; data not shown for U87MG).

A cell cycle analysis of D54MG, U87MG, and U373MG cultures labeled with propidium iodide and analyzed by flow cytometry showed that AAL881 treatment (5 $\mu\text{mol/L}$) resulted in a significant increase in the proportion of cells in the G₁ cell cycle fraction and decreased the proportion of cells in the G₂-M and S phases (Fig. 3A-C; data not shown for U373MG), consistent with G₁ cell cycle arrest. In addition, the antineoplastic activity of AAL881 seemed to be partially mediated through the induction of apoptosis as 5 $\mu\text{mol/L}$ of AAL881 showed a significant increase in apoptosis as shown by the Annexin-V assay (Fig. 3B, inset and D). Thus, AAL881 inhibits the growth of human glioma cell cultures with both antiproliferative and proapoptotic effects. In addition, the antiproliferative effect of AAL881 in glioma cell lines is independent from the levels of active B-RAF or C-RAF expression, as shown by a universal decrease in proliferation among D54MG, U87MG, and U373MG upon treatment with AAL881.

AAL881 inhibits proliferation of vascular endothelial cells and VEGF secretion from glioma. VEGF is a critical mediator of tumor angiogenesis. VEGF secreted from the tumor cells activates VEGFR2 (kinase insert domain receptor, KDR) on endothelial cells to promote vascular proliferation and survival. AAL881 effectively inhibited VEGF secretion measured by ELISA from D54MG cells in a concentration-dependent manner (Fig. 4A). In addition, AAL881 inhibited the proliferation of bovine aortic endothelial cells (Fig. 4B). Although these endothelial cells are not fully representative of tumor-derived microvessels, bovine aortic endothelial cells are regulated in a similar manner in response to growth factors. Thus, AAL881 shows the potential to disrupt both VEGF secretion in tumor cells and the proliferation of the target endothelial cells.

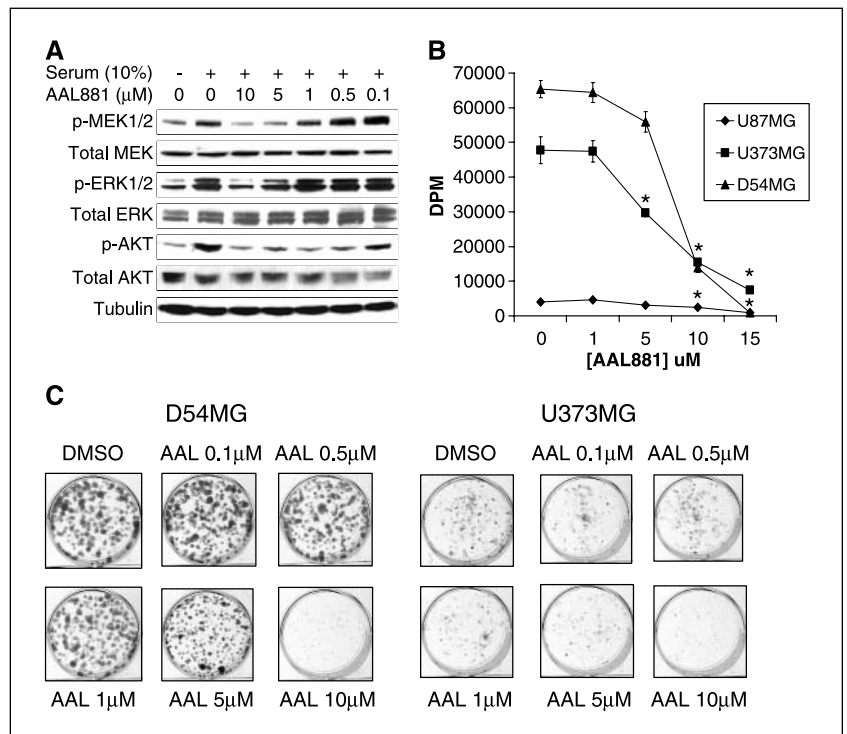
AAL881 blocks glioma invasion. Activated RAF facilitates cancer cell motility and invasion. Unlike most other types of cancer, the morbidity and mortality from most brain tumors come not from metastases, but rather, from local invasion of the tumor,

preventing complete surgical resection. Therefore, we investigated the effect of AAL881 on glioma cellular invasion using the well-studied Matrigel invasion assay in which tumor cells are permitted to invade through an artificial extracellular matrix. AAL881 at a concentration of 1 $\mu\text{mol/L}$ significantly blocked Matrigel invasion relative to an effect on motility (Fig. 4C and D). At higher concentrations (10 $\mu\text{mol/L}$), AAL881 dramatically inhibited both motility and invasion (Fig. 4C and D).

AAL881 inhibits tumor growth. Orally dosed AAL881 administered at 100 mg/kg per day for 10 doses was tolerated by tumor-bearing athymic mice without significant weight loss (data not shown). No toxic deaths were seen in mice treated with AAL881. As one mechanism of AAL881 involves the disruption of VEGFR activity, we examined the effects of AAL881 against a D54MG xenograft *in vivo*. Xenograft models permit the dissection of specific pathways in tumors derived from human patients. S.c. xenograft studies allow for the direct measurement of tumor volumes and acquisition of tumor tissue directly without restriction of drug delivery by the blood-brain barrier. An intracranial xenograft model permits examination of tumor growth in a native environment with cerebral vasculature that may be differentially regulated relative to systemic vasculature. Therefore, these models used in combination offer the greatest opportunity to quantify the antitumor properties of a drug.

In a heterotopic xenograft model of established s.c. tumors, AAL881 (100 mg/kg q.d. for a total of 10 days administered 5 days on/2 days off/5 days on) significantly slowed D54MG xenograft growth in three trials (representative results, Fig. 5A and B). As measured by time to reach five times the initial tumor volume, AAL881 delayed median tumor growth by >150 days ($P = 0.001$ compared with control). Sustained complete tumor regressions were seen with AAL881 therapy (5 of 10 treated animals in two studies, and 4 of 10 animals in a third study). No tumors that underwent complete regression redeveloped. Of note, we

Figure 2. AAL881 blocks measures of cellular proliferation in cell culture. **A**, AAL881 inhibited MEK, ERK, and Akt phosphorylation of human glioma D54MG cell lines. D54MG cultures were pretreated for 1 hour with increasing concentrations of AAL881 followed by 15 minutes of incubation with 10% serum. Whole cell lysates were collected, resolved by SDS-PAGE, and immunoblotted with phosphospecific antibodies. Membranes were stripped and reprobed with antibodies to measure total levels of each protein. Equal protein loading was confirmed by tubulin immunoblotting. **B**, AAL881 inhibited glioma cell proliferation in a concentration-dependent fashion. D54MG, U87MG, and U373MG cells were plated in 12-well plates at a cellular density of 10,000 cells/well. Cells were treated with AAL881 concentrations in quadruplicate wells for 48 hours in serum-fed conditions. Cells were labeled with [³H]thymidine for 4 hours, and then analyzed by scintillation (*, $P < 0.05$ compared with control). **C**, AAL881 induced a concentration-dependent decrease in colony formation. D54MG and U373MG cells were plated at a density of 500 cells/well in sextuplicate wells of six-well dishes and treated with control vehicle or increasing concentrations of AAL881 (0.1-10 $\mu\text{mol/L}$). Plates were incubated for 10 days and stained with Coomassie blue.



consistently detected populations of xenografts relatively resistant, growth retarded, or cured in response to AAL881 in each trial.

Survival of mice with implanted intracranial tumors is used as a clinical surrogate for tumor growth. In an intracranial D54MG xenograft study, AAL881 led to moderate increases in median animal life span in replicate studies (representative experiment shown in Fig. 5C) with median life spans of 12 days for control mice and 44 days for AAL881-treated animals ($P = 0.001$ compared with control). A minority of mice achieved long-term survival with AAL881 treatment (2 of 10 mice).

Immunohistochemical analysis of tumors treated with inhibitors. We examined the consequences of AAL881 treatment on the histologic appearance of established intracranial D54MG xenografts treated with a course of orally administered therapies. Mice with orthotopically implanted tumors were sacrificed immediately after the 10-day course of AAL881 treatment to determine the phenotypic effects of treatment. Sections of the brains from AAL881-treated animals were remarkable for unilat-

eral, intraparenchymal regions of acute coagulative necrosis (Fig. 6A). The pattern and distribution of the necrosis seen in the treated tumors correlated with the pattern and distribution of viable intraparenchymal tumor in the nontreated controls (Fig. 6A). Furthermore, the microscopic appearance of the necrotic nuclear debris revealed large nuclei, particularly along the necrosis-host brain interface. This feature, along with the observation of no intraparenchymal tumor in these mice with obvious overlying subarachnoid tumor strongly suggested the tissue undergoing coagulative necrosis was predominately, if not entirely, the xenografted neoplasm. The subarachnoid viable tumor found in the treated animals reflected the pattern and distribution of viable tumor that was frequently accompanied by underlying intraparenchymal tumor in the placebo-treated control brains. Sections of brain from control (DMSO treated) animals showed that acute coagulative necrosis was uncommonly encountered, although small foci of necrosis were present in all parenchymal tumors. Analysis of proliferation was complicated by the widespread necrosis within the treated tumors, with the rim of viable tumor still demonstrating a significant proliferative index (Fig. 6A). Furthermore, vascularity was absent in the necrotic areas of AAL881-treated tumors, as expected, but the surviving tumor rim did not show significant differences in tumor vascularity (as determined by CD31 and VEGFR-2 immunostaining) between control and AAL881-treated tumors in parallel with prior results with vascular disrupting agents (30).

Immunohistochemical analysis of a key intracellular mediator that contributes to the malignancy of gliomas was also done. Tumors grown in mice under control conditions displayed widespread and uniform expression of phosphorylated ERK1/2 consistent with the activation of this pathway. In contrast, mice treated with a single dose of AAL881 (100 mg/kg per gavage) displayed a nearly significant decrease in phosphorylated ERK1/2 at 6 hours ($P = 0.07$ compared with control) after treatment and a partial recovery at 16 hours after treatment (Fig. 6B). Of note, tumors harvested from vehicle-treated mice and AAL881-treated mice showed similar intensity and distribution of phosphorylated AKT (Fig. 6C).

Discussion

Survival of patients with malignant gliomas remains dismal despite current optimal treatments. Novel therapies targeting molecular changes in tumor cells may offer therapeutic benefits with limited toxicity (31). Several oncogenic pathways may be molecular targets useful in glioma therapy. RAF kinase, a downstream effector in the RAS signaling pathway, can drive tumor cellular proliferation. RAS effector pathways also promote angiogenesis through transcriptional up-regulation of angiogenic factors and increased invasiveness through ERK-mediated regulation of matrix metalloproteinases and RAC-mediated effects on the cytoskeleton (32). High ERK expression correlates with poor prognosis in patients with glioblastoma multiforme (33). Indirect inhibition of RAF kinase by FTIs has shown benefit in glioma xenograft models (34). Clinical studies using FTIs in gliomas have shown more modest benefits. In addition to targeting the growth pathways of cancer cells, a strategy to modify neoangiogenesis in the tumors is also important. VEGF is a potent angiogenic factor in malignant gliomas (35). Targeting VEGFR functions by monoclonal antibody or small molecule kinase inhibitors has been shown to decrease growth and angiogenesis

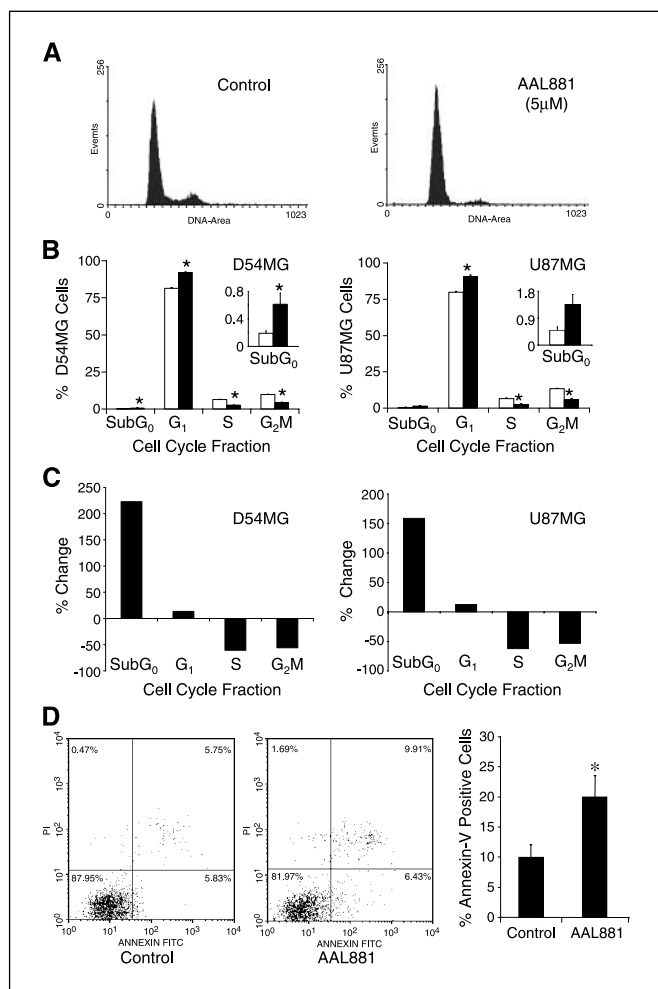
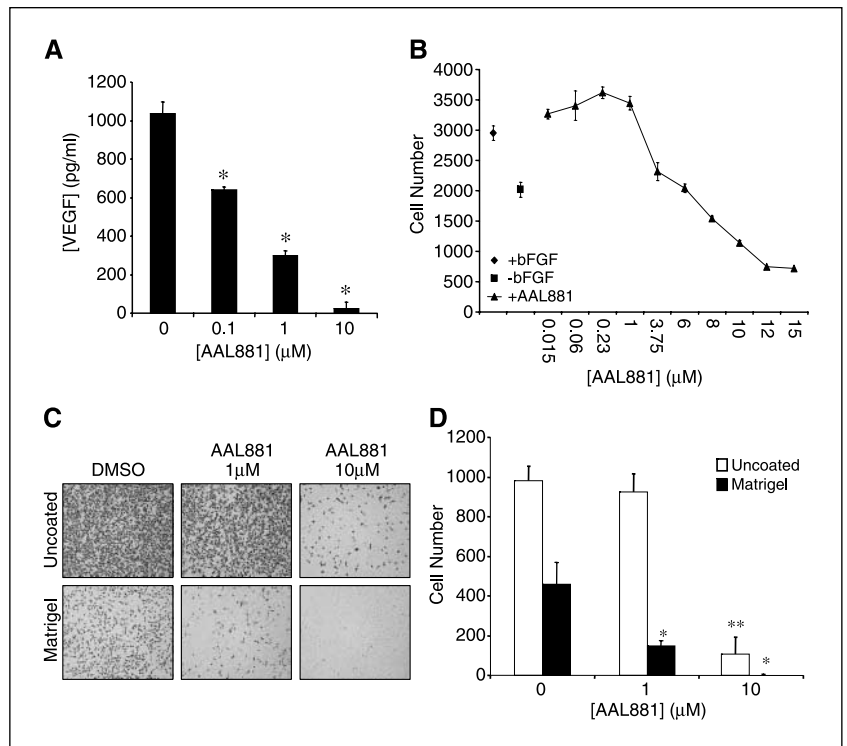


Figure 3. AAL881 induces cell cycle G₁ arrest with induction of apoptosis. A and B, D54MG, U87MG, and U373MG (data not shown) cultures were treated with either DMSO control (0.1%) or AAL881 (5 μ mol/L) for 48 hours, harvested, permeabilized with ethanol, and labeled with propidium iodide. Flow cytometric analysis of cell cycle fractions in D54MG and U87MG cells is shown (*, $P < 0.05$ compared with control). C, percentage of change in the cell cycle fraction of D54MG and U87MG cells after AAL881 treatment. D, AAL881 (5 μ mol/L) induces the apoptosis of D54MG cells as shown by a significant increase in Annexin V staining (*, $P = 0.014$).

Figure 4. AAL881 inhibits tumor cell VEGF expression and invasion and endothelial cell proliferation. *A*, VEGF was quantified from supernatants of either control (DMSO) or AAL881-treated D54MG cells using VEGF ELISA-Quantikine assay (R&D Systems). AAL881 inhibited VEGF secretion from D54MG cells in a concentration-dependent manner (*, $P < 0.01$ compared with control). *B*, bovine endothelial cells increased proliferation after bFGF administration. AAL881 inhibited the proliferation of bovine aortic endothelial cells in a dose-dependent manner in the presence of bFGF. *C* and *D*, Matrigel invasion assays were purchased from BD Biosciences and used according to instructions. Cells on inserts were fixed and stained 48 hours after plating. Cells were counted manually with 20 fields per data point (*, $P < 0.01$ compared with control invasion through uncoated membranes). AAL881 at 1 $\mu\text{mol/L}$ significantly inhibits invasion of tumor cells as illustrated by the decreased number of cells on Matrigel-coated inserts. AAL881 at 10 $\mu\text{mol/L}$ inhibits both the motility/migration and invasion as illustrated by the decreased number of cells on uncoated inserts and near absence of cells on Matrigel-coated inserts.



and reverse the radioresistance of gliomas (36–40). Therefore, an agent with dual action against both RAF and VEGFR kinases might offer additional benefits for tumor control.

We now report that a novel small molecule inhibitor targeting both RAF and VEGFR kinases, AAL881, displays significant activity against a well-characterized malignant glioma cell line and xenograft. To date, malignant glioma cell lines have shown relative resistance to small molecule antagonists directed towards oncogenic pathways. D54MG xenografts are relatively insensitive to low-molecular weight tyrosine kinase inhibitors that specifi-

cally target VEGFR function (data not shown). Thus, the activity of AAL881 against D54MG suggests that either RAF activity is critical to tumor cell growth or that the joint disruption of RAF and VEGF pathways creates a combinatorial benefit. As we detected both direct effects suppressing ERK and AKT as well as *in vivo* antiangiogenic effects, AAL881 may have distinct therapeutic advantages over the use of FTIs which may only partially target RAS activity as some RAS family members are geranylgeranylated. In addition, targeting the MEK/ERK pathway at the RAF level may be particularly useful because RAF is a key

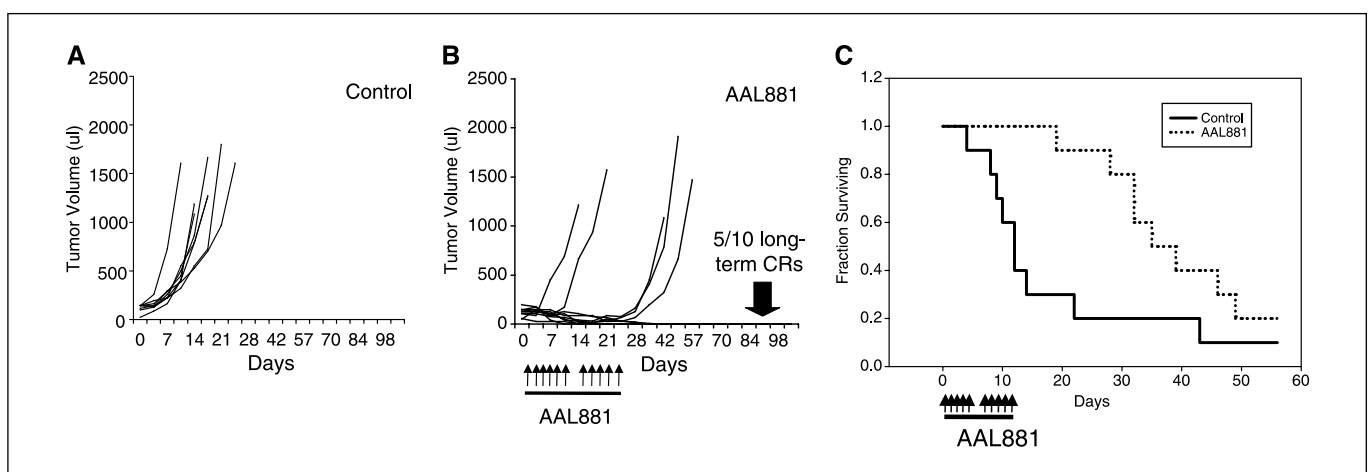


Figure 5. AAL881 induces control of glioma tumor growth. *A* and *B*, D54MG xenografts were grown in the flanks of athymic nude mice until a tumor volume of 100 to 300 mm^3 was reached. Animals were treated per gavage with AAL881 (100 mg/kg q.d.) for 5 days, followed by 2 days off, then for an additional 5 days. Tumor volume was also measured with calipers twice a week. Tumor volume was calculated by the formula: volume = [(smallest diameter² × largest diameter) / 2]. Treatment of mice with established s.c. glioma xenografts with AAL881 not only significantly delayed tumor growth in 5 out of 10 mice ($P < 0.001$), but also cured 5 out of 10 mice in repeated trials. *C*, AAL881 increased the survival of nude athymic mice bearing intracranial glioma tumors. D54MG xenografts were implanted into these mice. After 3 days, animals were treated per gavage with AAL881 (100 mg/kg q.d. × 10 doses). AAL881 significantly increased median survival with a median increase from 12 days (control) to 44 days (AAL881; $P = 0.001$ compared with control).

regulator of the MEK/ERK pathway, whereas other upstream targets such as the growth factor ligands, receptor tyrosine kinases, and even RAS have many other potential effectors. AAL881 had antiproliferative effects not only by arresting the cell cycle progression, but also by inducing apoptosis. Of some surprise, AAL881 decreased the *in vitro* activation of AKT, a mediator of the PI3K pathway, which may explain a component of the proapoptotic effects of AAL881. Although RAS activates PI3K, and thus, AKT, RAF activity is less clearly linked to AKT activation. Therefore, the decrease in AKT phosphorylation after AAL881 treatment may either denote that RAF activates AKT in these cells or that AAL881 may generate off-target effects. Despite the distinct *in vitro* inhibition of AKT by AAL881, intracranial tumors from AAL881-treated mice did not show a decrease in AKT phosphorylation. These results are consistent with our recently published studies (27, 28) in which targeted therapies effectively block AKT activity in cell culture but not in xenografts, whereas

ERK activity is more resistant in cell culture studies but is more readily targeted in xenografts, suggesting that caution should be applied when extrapolating from lessons derived from cell culture studies alone, especially with therapies that have antiangiogenic activity. Additionally, the relative resistance of AKT phosphorylation with AAL881 treatment suggests that AAL881 may offer combinatorial benefit with agents targeting PI3K or downstream pathways. Furthermore, AAL881 inhibited tumor cell motility and invasion, important phenotypes of malignant gliomas that often cause failure of local therapy.

Tumor growth is critically dependent on the development of neoangiogenic blood vessels through tumor cell and stromal elaboration of angiogenic factors, including VEGF, which act on tumor-associated endothelial cells that express VEGF receptors to stimulate endothelial cell proliferation and vascular formation. AAL881 exhibited the ability to block angiogenesis at two levels—the upstream production of proangiogenic growth factors from the

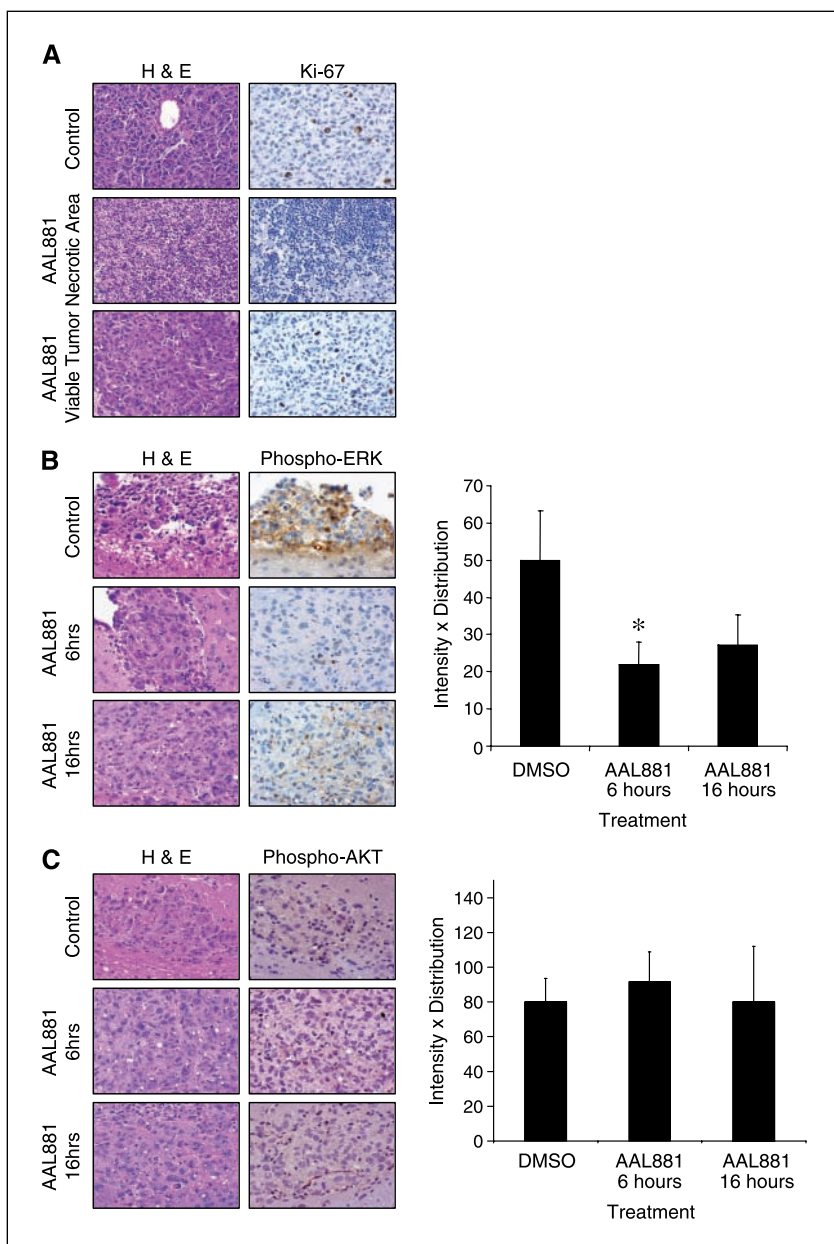


Figure 6. Histopathologic findings of AAL881-treated orthotopic tumor xenografts. *A*, nude athymic mice with established D54MG xenografts were treated with vehicle control or AAL881 (100 mg/kg/d) per gavage for 5 days. Three hours after the final dose, tumors were harvested and formalin fixed, and then stained for H&E and Ki-67. Tumor from untreated control mouse showed hypercellularity with nuclear pleomorphism and vascular proliferation. Ki-67-positive cells (brown). Tumor from AAL881-treated mice showed a large area of coagulative necrosis without any Ki-67 staining. Viable tumors from AAL881-treated mice were found predominantly in the leptomeningeal space with Ki-67-positive cells that are not different from the vehicle-treated control mice. *B* and *C*, nude athymic mice were intracranially implanted with D54MG tumor. Ten days after implantation, mice were treated with vehicle control or AAL881 (100 mg/kg) per gavage. Tumors were then harvested at 6 and 16 hours after drug administration. Tumor samples were formalin-fixed, and stained with phosphospecific ERK1/2 (p-ERK) antibody (*B*) and phosphospecific AKT (p-AKT) antibody (*C*). *B*, tumor from vehicle-treated control mice showed widespread and intense staining of p-ERK, whereas tumor from AAL881-treated mice displayed a trend towards significant decrease in phosphorylated ERK1/2 at 6 hours after treatment (*, $P = 0.07$ compared with control) and partial recovery at 16 hours after treatment. *C*, tumor from vehicle-treated control mice and AAL881-treated mice displayed similar intensity and distribution of p-AKT staining.

tumor cells and the downstream activity of VEGF on the target endothelial cells. In addition, disruption of the RAF-MEK-ERK pathway in tumor cells may down-regulate the secretion of not only VEGF but also other proangiogenic factors such as transforming growth factor- α and basic fibroblast growth factor. The *in vivo* antiangiogenic effects seen in our experiment are consistent with those seen in other vascular disruption agents, which showed widespread necrotic death of intraparenchymal tumor and preservation of tumor in areas of greater baseline vasculature such as the meninges (30, 39).

AAL881 displays potent effects on cellular proliferation and invasion and VEGF secretion relative to other low-molecular weight inhibitors directed against EGFR, PDGFR, VEGFR, and mammalian target of rapamycin in these same cell lines (data not shown). Other inhibitors have required 5- to 10-fold greater concentrations to achieve similar efficacies in these assays. The striking potency of AAL881 is also additionally in *in vivo* studies against glioma xenografts grown in both flank and the intracranial locations. AAL881 induced and maintained complete responses in a subset of treated animals—an effect that we have not detected with other low-molecular weight inhibitors of signal transduction pathways in this model. A low-molecular weight VEGFR2/PDGFR antagonist had essentially no efficacy against these same xenografts (data not shown), suggesting either that RAF is the effective target of AAL881 or that the dual targeting of VEGFR and RAF is required for efficacy. RAF represents a dual compartment target itself as we have shown that tumor cells themselves respond to AAL881 and tumor-associated endothelial cells can be inhibited by RAF-targeting strategies. Although another VEGFR/RAF inhibitor, sorafenib (BAY 43-9006, Bayer Pharmaceuticals, NY) is in both preclinical and clinical development for solid cancers including gliomas in our laboratory, the efficacy of this agent against RAF itself remains controversial (41, 42). Thus, AAL881 may show differential efficacy relative to sorafenib even in cancers without activating mutations in either RAS or RAF family members.

Future development of AAL881 for targeting gliomas will require improved characterization of the ability of this agent to

penetrate the blood-brain barrier. Although we have detected the activity of AAL881 against an orthotopic intracranial model, this model does not fully recapitulate the invasive phenotype of gliomas associated with tumor cells protected by an intact blood-brain barrier. However, AAL881 faces a distinct advantage in that tumor-associated vasculature is a primary target of both RAF and VEGF inhibition, suggesting that AAL881 may exhibit activity independent from delivery into brain parenchyma by acting on the abluminal side of blood vessels. We have identified direct downstream targets that are inhibited in parallel to the antiproliferative effects of AAL881, suggesting the potential utility of phosphorylated ERK as molecular markers that can be used in pharmacodynamic studies in which glioma patients with recurrent tumor can be treated with a course of AAL881 prior to surgical resection. Despite the activity of this agent in preclinical trials, the genetic diversity of malignant gliomas suggests that either long-term efficacy of any targeted therapy will require patient selection or combination with other targeted agents. In conclusion, this is the first report of successful treatment using a dual RAF and VEGFR kinase inhibitor in glioma xenograft models and suggests that a clinical trial in patients with malignant gliomas may be warranted.

Acknowledgments

Received 1/24/2006; revised 6/2/2006; accepted 6/29/2006.

Grant support: Pediatric Brain Tumor Foundation of the United States, Accelerate Brain Cancer Cure, Childhood Brain Tumor Foundation (J.N. Rich), and Southeastern Brain Tumor Foundation funds (A.B. Hjelmeland). This work was also supported by NIH grants NS047409, NS054276, and 1 P50 CA 108786 (J.N. Rich), and NIH grants NS20023 and CA11898 and NIH grant M01 RR 30, GCRC Program, National Center for Research Resources, National Cancer Institute Specialized Programs of Research Excellence 1 P20 CA096890, FCG grants, and a grant from the Pediatric Brain Tumor Foundation of the United States (D.D. Bigner). A.B. Hjelmeland is a Paul Brazen/American Brain Tumor Association Fellow. J.N. Rich is a Damon Runyon-Lilly Clinical Investigator supported by the Damon Runyon Cancer Research Foundation and a Sidney Kimmel Cancer Foundation Translational Scholar.

The costs of publication of this article were defrayed in part by the payment of page charges. This article must therefore be hereby marked *advertisement* in accordance with 18 U.S.C. Section 1734 solely to indicate this fact.

The authors thank Qiulian Wu, Qing Shi, and Kate Vredenburg for technical and editorial assistance.

References

1. Scott CB, Scarantino C, Urtasun R, et al. Validation and predictive power of Radiation Therapy Oncology Group (RTOG) recursive partitioning analysis classes for malignant glioma patients: a report using RTOG 90-06. *Int J Radiat Oncol Biol Phys* 1998;40:51-5.
2. LaRocca RV, Rosenblum M, Westermark B, Israel MA. Patterns of proto-oncogene expression in human glioma cell lines. *J Neurosci Res* 1989;24:97-106.
3. Blin N, Muller-Brechlin R, Carstens C, Meese E, Zang KD. Enhanced expression of four cellular oncogenes in a human glioblastoma cell line. *Cancer Genet Cytogenet* 1987;25:285-92.
4. Arvanitis D, Malliri A, Antoniou D, et al. Ras p21 expression in brain tumors: elevated expression in malignant astrocytomas and glioblastomas multiforme. *In Vivo* 1991;5:317-21.
5. James GL, Goldstein JL, Brown MS, et al. Benzodiazepine peptidomimetics: potent inhibitors of Ras farnesylation in animal cells. *Science* 1993;260:1937-42.
6. Kohl NE, Mosser SD, deSolms SJ, et al. Selective inhibition of ras-dependent transformation by a farnesyltransferase inhibitor. *Science* 1993;260:1934-7.
7. Schlessinger J. Cell signaling by receptor tyrosine kinases. *Cell* 2000;103:211-25.
8. Lokker NA, Sullivan CM, Hollenbach SJ, Israel MA, Giese NA. Platelet-derived growth factor (PDGF) autocrine signaling regulates survival and mitogenic pathways in glioblastoma cells: evidence that the novel PDGF-D ligands may play a role in the development of brain tumors. *Cancer Res* 2002;62:3729-35.
9. Meadows KN, Bryant P, Pumiglia K. Vascular endothelial growth factor induction of the angiogenic phenotype requires Ras activation. *J Biol Chem* 2001; 276:49289-98.
10. Rich JN, Guo C, McLendon RE, Bigner DD, Wang XF, Counter CM. A genetically tractable model of human glioma formation. *Cancer Res* 2001;61:3556-60.
11. Sonoda Y, Ozawa T, Hirose Y, et al. Formation of intracranial tumors by genetically modified human astrocytes defines four pathways critical in the development of human anaplastic astrocytoma. *Cancer Res* 2001;61:4956-60.
12. Guha A, Feldkamp MM, Lau N, Boss G, Pawson A. Proliferation of human malignant astrocytomas is dependent on Ras activation. *Oncogene* 1997;15:2755-65.
13. Holland EC, Celestino J, Dai C, Schaefer L, Sawaya RE, Fuller GN. Combined activation of Ras and Akt in neural progenitors induces glioblastoma formation in mice. *Nat Genet* 2000;25:55-7.
14. Bredel M, Pollack IF, Freund JM, Hamilton AD, Sebt SM. Inhibition of Ras and related G-proteins as a therapeutic strategy for blocking malignant glioma growth. *Neurosurgery* 1998;43:124-31.
15. Pollack IF, Bredel M, Erff M, Hamilton AD, Sebt SM. Inhibition of Ras and related guanosine triphosphate-dependent proteins as a therapeutic strategy for blocking malignant glioma growth. II. Preclinical studies in a nude mouse model. *Neurosurgery* 1999;45:1208-14.
16. Lebowitz PF, Casey PJ, Prendergast GC, Thissen JA. Farnesyltransferase inhibitors alter the prenylation and growth-stimulating function of RhoB. *J Biol Chem* 1997; 272:15591-4.
17. Crespo NC, Ohkanda J, Yen TJ, Hamilton AD, Sebt SM. The farnesyltransferase inhibitor, FTI-2153, blocks bipolar spindle formation and chromosome alignment and causes prometaphase accumulation during mitosis of human lung cancer cells. *J Biol Chem* 2001;276: 16161-7.
18. Delmas C, Heliez C, Cohen-Jonathan E, et al. Farnesyltransferase inhibitor, R115777, reverses the resistance of human glioma cell lines to ionizing radiation. *Int J Cancer* 2002;100:43-8.
19. Glass TL, Liu TJ, Yung WK. Inhibition of cell growth in human glioblastoma cell lines by farnesyltransferase inhibitor SCH66336. *Neuro-oncol* 2000;2:151-8.
20. Cloughesy TF, Kuhn J, Robins HI, et al. Phase I trial of

- tipifarnib in patients with recurrent malignant glioma taking enzyme-inducing antiepileptic drugs: a North American Brain Tumor Consortium Study. *J Clin Oncol* 2005;23:6647-56.
21. Chakravarti A, Zhai G, Suzuki Y, et al. The prognostic significance of phosphatidylinositol 3-kinase pathway activation in human gliomas. *J Clin Oncol* 2004;22:1926-33.
22. Knobbe CB, Reifenberger J, Reifenberger G. Mutation analysis of the Ras pathway genes NRAS, HRAS, KRAS and BRAF in glioblastomas. *Acta Neuropathol (Berl)* 2004;108:467-70.
23. Basto D, Trovisco V, Lopes JM, et al. Mutation analysis of B-RAF gene in human gliomas. *Acta Neuropathol (Berl)* 2005;109:207-10.
24. Davies H, Bignell GR, Cox C, et al. Mutations of BRAF gene in human cancer. *Nature* 2002;417:949-54.
25. O'Reilly MS, Holmgren L, Shing Y, et al. Angiostatin: a novel angiogenesis inhibitor that mediates the suppression of metastases by a Lewis lung carcinoma. *Cell* 1994; 79:315-28.
26. Friedman HS, Schold SC, Jr., Bigner DD. Chemotherapy of subcutaneous and intracranial human medulloblastoma xenografts in athymic nude mice. *Cancer Res* 1986;46:224-8.
27. Goudar RK, Shi Q, Hjelmeland MD, et al. Combination therapy of inhibitors of epidermal growth factor receptor/vascular endothelial growth factor receptor 2 (AEE788) and the mammalian target of rapamycin (RAD001) offers improved glioblastoma tumor growth inhibition. *Mol Cancer Ther* 2005;4:101-12.
28. Rich JN, Sathornsumetee S, Keir ST, et al. ZD6474, a novel tyrosine kinase inhibitor of vascular endothelial growth factor receptor and epidermal growth factor receptor, inhibits tumor growth of multiple nervous system tumors. *Clin Cancer Res* 2005;11:8145-57.
29. McLendon RE, Wikstrand CJ, Matthews MR, Al-Baradei R, Bigner SH, Bigner DD. Glioma associated antigen expression in oligodendroglial neoplasms: tenascin and epidermal growth factor receptor. *J Histochem Cytochem* 2000;48:1103-10.
30. Tozer GM, Kanthou C, Baguley BC. Disrupting tumour blood vessels. *Nat Rev Cancer* 2005;5:423-35.
31. Rich JN, Bigner DD. Development of novel targeted therapies in the treatment of malignant glioma. *Nat Rev Drug Discov* 2004;3:430-46.
32. Downward J. Targeting RAS signaling pathways in cancer therapy. *Nat Rev Cancer* 2003;3:11-22.
33. Mawrin C, Dietsch S, Treuheit T, et al. Prognostic relevance of MAPK expression in glioblastoma multiforme. *Int J Oncol* 2003;23:641-8.
34. Feldkamp MM, Lau N, Guha A. Growth inhibition of astrocytoma cells by farnesyl transferase inhibitors is mediated by a combination of anti-proliferative, proapoptotic and anti-angiogenic effects. *Oncogene* 1999; 18:7514-26.
35. Plate KH, Breier G, Weich HA, Risau W. Vascular endothelial growth factor is a potential tumor angiogenesis factor in human gliomas *in vivo*. *Nature* 1992; 359:845-8.
36. Laird AD, Vajkoczy P, Shawver LK, et al. SU6668 is a potent antiangiogenic and antitumor agent that induces regression of established tumors. *Cancer Res* 2000;60: 4152-60.
37. Goldbrunner RH, Bendszus M, Wood J, Kiderlen M, Sasaki M, Tonn JC. PTK787/ZK222584, an inhibitor of vascular endothelial growth factor receptor tyrosine kinases, decreases glioma growth and vascularization. *Neurosurgery* 2004;55:426-32.
38. Geng L, Donnelly E, McMahon G, et al. Inhibition of vascular endothelial growth factor receptor signaling leads to reversal of tumor resistance to radiotherapy. *Cancer Res* 2001;61:2413-9.
39. Kunkel P, Ulbricht U, Bohlen P, et al. Inhibition of glioma angiogenesis and growth *in vivo* by systemic treatment with a monoclonal antibody against vascular endothelial growth factor receptor-2. *Cancer Res* 2001; 61:6624-8.
40. Kozin SV, Boucher Y, Hicklin DJ, Bohlen P, Jain RK, Suit HD. Vascular endothelial growth factor receptor-2 blocking antibody potentiates radiation-induced long-term control of human tumor xenografts. *Cancer Res* 2001;61:39-44.
41. Wilhelm SM, Carter C, Tang L, et al. BAY 43-9006 exhibits broad spectrum oral antitumor activity and targets the RAF/MEK/ERK pathway and receptor tyrosine kinases involved in tumor progression and angiogenesis. *Cancer Res* 2004;64:7099-109.
42. Strumberg D, Richly H, Hilger RA, et al. Phase I clinical and pharmacokinetic study of the novel Raf kinase and vascular endothelial growth factor receptor inhibitor BAY 43-9006 in patients with advanced refractory solid tumors. *J Clin Oncol* 2005;23:965-72.